

PHYSICAL REVIEW A

GENERAL PHYSICS

THIRD SERIES, VOLUME 27, NUMBER 4

APRIL 1983

Theoretical study of the lowest $1\Sigma_g^+$ doubly excited state of H_2

A. U. Hazi

Lawrence Livermore National Laboratory, University of California, Livermore, California 94550

C. Derkits and J. N. Bardsley

Physics Department, University of Pittsburgh, Pittsburgh, Pennsylvania 15260

(Received 30 August 1982)

The energy and width of the $1\sigma_u^2 1\Sigma_g^+$ state of H_2 are calculated using Feshbach projection operators and the Stieltjes moment method. The results are compared with an analysis of the double minima in the potential-energy curves of the $1\Sigma_g^+$ Rydberg states. The doubly excited $1\sigma_u^2$ configuration is unstable with respect to autoionization for $R < 2.65a_0$, and the autoionization rate is sensitive to both the value of the internuclear separation and the energy of the emitted electron.

I. INTRODUCTION

The $1\sigma_u^2 1\Sigma_g^+$ configuration of H_2 has long been of interest since it is the lowest doubly excited configuration in the hydrogen molecule. Its existence leads to the well-known double minima in the potential-energy curves of the excited $1\Sigma_g^+$ states such as the *EF* and *GK* states. For example, at small internuclear distance R the *EF*-state wave function is dominated by the configuration $1\sigma_g 2\sigma_g$ whereas near the outer minimum the $1\sigma_u^2$ configuration is more important. At very large separations, a single configuration cannot suffice to describe the proper asymptotic limit. At small R the energy of the $1\sigma_u^2$ configuration is larger than that of the $H_2^+ 2\Sigma_g^+$ ground state, so that the doubly excited state is embedded in an electron-scattering continuum and can decay by autoionization. Its properties in this autoionization region are of special interest with regard to a wide variety of collision phenomena. For example, recombination of low-energy electrons and H_2^+ ions in low vibrational states proceeds primarily through the formation and subsequent dissociation of this state.

There have been several calculations of the potential-energy curve and autoionization lifetime, or width, of the $1\sigma_u^2 1\Sigma_g^+$ state. Although there is good agreement concerning the potential curve, the

calculated widths differ significantly. One approach is through the introduction of Feshbach¹ projection operators P and Q , chosen so that the spectrum of QHQ is discrete in the energy range of interest. The potential curve can then be obtained from the eigenvalues of QHQ , and the width from matrix elements of PHQ . This technique has been applied by Bottcher and Docken,² Rai Dastidar and Rai Dastidar,³ and very recently by Sato and Hara.⁴ In the two earlier papers,^{2,3} the open channel component $P\Psi$ was approximated by a simple product of a Coulomb wave function and an H_2^+ orbital. The calculated widths peak near $R = 1.6a_0$ with maximum values of 1 and 10 eV, respectively, and then decrease to 0.025 (Ref. 2) and 0 eV (Ref. 3) at the stabilization point $R_s = 2.8a_0$, where the potential curve of $1\sigma_u^2$ crosses that of the ground electronic state of H_2^+ . In contrast to the situation pertaining to unstable negative ions, the autoionization widths for neutral states should approach a nonzero limit as $R \rightarrow R_s$. The zero limit obtained by Rai Dastidar and Rai Dastidar³ does not appear to arise from any physical approximation that they made, but is probably due to numerical inaccuracies, or an inappropriate extrapolation. Sato and Hara⁴ have used a static-exchange approximation for the open-channel function $P\Psi$ and obtained a width which increases monotonically with increasing values of R . Thus,

their findings disagree seriously with the results of the earlier projection-operator calculations.^{2,3}

An alternative approach is to study the scattering of electrons by H_2^+ ions with fixed nuclei. The $1\sigma_u^2\ ^1\Sigma_g^+$ state then should appear as a resonance, with parameters that can be deduced from the energy dependence of the eigenphase shifts or S -matrix elements. Robb⁵ has performed close-coupling calculations for separations of $1.4a_0$, $2.0a_0$, and $2.6a_0$, and found a resonance at energies close to the predictions of Bottcher and Docken.² However, the width increases steadily from 0.65 eV at $1.4a_0$ to 1.9 eV at $2.6a_0$. A similar behavior was found in algebraic variational calculations by Takagi and Nakamura,⁶ and in subsequent four-state close-coupling calculations by Collins and Schneider.⁷

Perhaps the most intriguing and difficult method available for the calculation of autoionization widths is the complex-coordinate method. There has been considerable debate concerning the implementation of this approach for molecular systems.⁸ Using relatively simple wave functions, Moiseyev and Corcoran⁹ obtained a width of 1.2 eV at $R=1.4a_0$, which is approximately a factor of 2 larger than the values obtained in $e + H_2^+$ scattering calculations.⁵⁻⁷

The large degree of disagreement between these results is disturbing. In view of the uncertainty in both the magnitude and R dependence of the width of the $1\sigma_u^2\ ^1\Sigma_g^+$ state, we deemed it to be worthwhile to obtain independent estimates of this parameter before embarking upon calculations of dissociative recombination cross sections that will be reported in a subsequent paper.

In Sec. II, we will describe calculations within the Feshbach formalism¹ in which the widths are calculated using Stieltjes moment theory.¹⁰⁻¹² This technique can be applied to the calculation of any matrix element between a discrete state, represented by a square-integrable (L^2) function and a continuum function. It involves the replacement of the continuum by a large set of L^2 functions whose energy spectrum is distributed reasonably uniformly over the energy range of interest. It is applied here to the calculation of the matrix element $\langle \Psi | QHP | \Psi \rangle$, which determines the autoionization width.

In Sec. III, we will analyze the shape of the double minima in the potential-energy curves of the excited $^1\Sigma_g^+$ states of H_2 and will attempt to deduce the energies of the Rydberg and nonRydberg configurations and the strength of the coupling between them. This will give us information about the $1\sigma_u^2$ configuration at internuclear separations around $3a_0$. The requirement of continuity of the properties of this state at $R=R_s$ will then guide us in the choice of a potential curve and width in the autoion-

izing region ($R < R_s$), which will be used to calculate the cross sections for dissociative recombination and vibrational excitation in $e-H_2^+$ collisions in a subsequent paper.¹³

II. APPLICATION OF STIELTJES MOMENT THEORY

We have used configuration-interaction (CI) wave functions and the Stieltjes moment theory technique¹⁰⁻¹² to calculate the potential-energy curve and the autoionization width of the $1\sigma_u^2\ ^1\Sigma_g^+$ state at internuclear distances where it is unstable with respect to electron ejection. The method is based on projection-operator techniques and a golden-rule definition of the resonance width.¹ Discrete, square-integrable, many-electron basis functions (configurations) are used to expand the wave functions of *both* the resonance and the nonresonant scattering continuum. The Stieltjes moment theory is employed to extract a continuous approximation for the width $\Gamma(E)$ from the discrete representation of the background scattering. The present calculations of the $^1\Sigma_g^+$ state are similar to those reported previously^{11,12} for $1\sigma_u2\sigma_g\ ^1\Sigma_u^+$ and $1\sigma_u1\pi_g\ ^1\Pi_u$ doubly excited states.

The molecular-orbital basis set contained two groups of orbitals. The first group consisted of $7\sigma_g$, $6\sigma_u$, $4\pi_g$, and $4\pi_u$ orbitals which were linear combinations of contracted Cartesian Gaussian functions located on the two nuclei.¹⁴ The $1\sigma_g$ and $1\sigma_u$ orbitals corresponded to the two lowest states of H_2^+ , whereas the other orbitals were chosen to represent the other low-lying excited states of H_2^+ . For $R=1.4a_0$ and $2.0a_0$, the calculated and the exact energies of the $1\sigma_g$ orbital differed by less than 1 mhartree, whereas the difference was about twice as large for $R \geq 2.5a_0$. The orbital basis set was sufficiently flexible to produce reasonable descriptions of the $1\sigma_g^2$ and $1\sigma_u^2\ ^1\Sigma_g^+$ states. The difference between our calculated and the exact energies¹⁵ of the $^1\Sigma_g^+$ ground state varied from 13 mhartree at $R=1.4a_0$ to 2 mhartree at $R=4.0a_0$. This is reasonable, given that the orbital basis was optimized for the excited states of H_2 . For internuclear distances less than $2.8a_0$, the $1\sigma_u^2$ state can autoionize into the $1\sigma_gk\sigma_g\ ^1\Sigma_g^+$ continuum. Since the ejected electron has σ_g symmetry, the second group of orbitals was chosen to contain $6s$ and $10d\sigma_g$ Gaussian functions located on the center of the molecule. These functions had a geometric sequence of orbital exponents¹⁶ ($s=0.06, 0.03, 0.008, 0.004, 0.002, 0.001$; $d=0.52, 0.26, 0.128, 0.064, 0.032, 0.016, 0.008, 0.004, 0.002, 0.001$), and they were Schmidt orthogonalized sequentially to the other seven σ_g orbitals.

The total CI space (resonant plus nonresonant

parts) contained all the 337 $^1\Sigma_g^+$ configurations which could be constructed from the full basis of $23\sigma_g$, $6\sigma_u$, $4\pi_g$, and $4\pi_u$ orbitals. We have carried out two series of calculations with this configuration list but with different definitions of the resonant subspace Q_0 . Since the $1\sigma_u^2\ ^1\Sigma_g^+$ state autoionizes into a single electronic channel corresponding to $H_2^+ \ ^2\Sigma_g^+ + e^-(k\sigma_g)$, the configurations $1\sigma_g n\sigma_g$, $n=1, \dots, 23$, were chosen to define the initial nonresonant subspace P_0 . The $1\sigma_u^2$ resonance was obtained as the lowest eigenstate of the Hamiltonian matrix constructed in the basis of the remaining 314 configurations (Q_0 space). Since the basis gave a reasonably good description of the three lowest members of the $^1\Sigma_g^+$ autoionizing Rydberg series converging to the $1\sigma_u^2\ ^2\Sigma_u^+$ state of H_2^+ , we chose all three resonances to define the resonant subspace:

$$Q = \sum_{i=1}^3 |\phi_{ir}\rangle \langle \phi_{ir}|.$$

The fully correlated nonresonant scattering solutions were obtained by diagonalizing the Hamiltonian in the 334-dimensional subspace orthogonal to Q . These calculations will be denoted as CI-A.

There is one difficulty with the definition of the subspaces P_0 and Q_0 in CI-A. The single configuration $1\sigma_u^2$, where $1\sigma_u \rightarrow (1s_A - 1s_B)$ asymptotically, does not dissociate properly at large internuclear separations. Formally, a two-configuration wave function containing $1\sigma_g^2$ and $1\sigma_u^2$ is required for correct dissociation.¹⁷ Since the configuration $1\sigma_g^2$ was included in the *nonresonant* subspace in calculation CI-A, the resulting $^1\Sigma_g^+$ resonance may not behave correctly at large internuclear distances. To remedy this difficulty, we performed a second set of calculations, denoted CI-B, in which $1\sigma_g^2$ was included in the resonant subspace Q_0 , i.e., the subspace P_0 consisted of only $1\sigma_g n\sigma_g$, $n=2, \dots, 23$. In this case, the $1\sigma_u^2$ resonance was obtained as the *second* lowest eigenstate of the 315×315 matrix $Q_0 H Q_0$, the lowest being an approximation to the $X^1\Sigma_g^+$ ground state. We then used the same procedure as in CI-A to determine the nonresonant scattering solutions.

The calculations were done at five internuclear separations R between $1.4a_0$ and $4.0a_0$. At a given value of R , the energy-dependent resonance width $\Gamma(E, R)$ was computed from the matrix elements coupling the $^1\Sigma_g^+$ doubly excited state to the discrete, nonresonant solutions using the Stieltjes moment theory technique. We employed both the original prescription of Langhoff¹⁸ and the algorithm of Hazi and Rescigno¹⁹ to obtain internally consistent approximations to Γ . The latter procedure involves fitting a histogram representation of

the indefinite integral $\int^E \Gamma(E', R) dE'$ to a power series in E^{-1} and differentiating the result analytically to obtain Γ as a continuous function of the ejected electron energy E . Figure 1 shows some typical results for $\Gamma(E, R)$ obtained with CI-A at $R=1.4a_0$. The width is plotted as a function of the total energy relative to the ground vibrational state of $H_2 \ X^1\Sigma_g^+$. The ejected electron energy can be obtained by subtracting the energy of $H_2^+ \ ^2\Sigma_g^+$, 16.18 eV at $R=1.4a_0$, from the total energy.

In a one-center expansion of the ejected electron wave function $k\sigma_g$, the $l=0$ (*s*-wave) and $l=2$ (*d*-wave) components are the most important² with a non-negligible contribution from higher partial waves at larger R values. While it was possible to compute fairly accurate values of the total width, the present σ_g basis set was not large enough to obtain accurate values for the partial widths. However, a crude estimate of the *d*-wave/*s*-wave branching ratio gave approximately 5/1 at $R=1.4a_0$ and 15/1 at $R=2.5a_0$. This is the trend one would expect with increasing internuclear distance. The "noise" in the discrete Stieltjes data of Fig. 1, which is typical of what we have found in all the calculations, is due indirectly to this large branching ratio. Some of the discrete eigenfunctions representing the $1\sigma_g k\sigma_g$ continuum have large *s*-wave components and others large *d*-wave components. Since these two types of solutions are intermingled in the pseudospectrum,

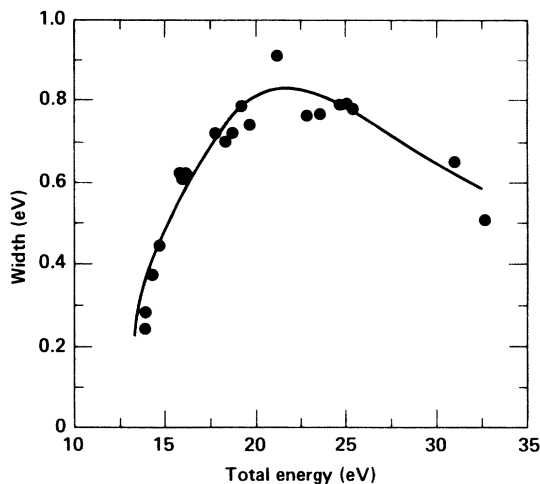


FIG. 1. Energy dependence of the fixed-nuclei resonance width $\Gamma(E, R)$ calculated with CI-A at $R=1.4a_0$ for $1\sigma_u^2\ ^1\Sigma_g^+$. Total energy is the sum of the ejected-electron energy E and the energy of $H_2^+ \ ^2\Sigma_g^+$ (16.18 eV at 1.4 bohr) relative to the ground vibrational state of H_2 . Points represent Stieltjes data and solid line denotes analytical approximation to $\Gamma(E, R)$ (see text).

and because the $1\sigma_u^2$ state couples preferentially to the d -wave portion of the continuum, the width matrix elements fluctuate between large and small values with increasing energy. As Fig. 1 shows, the moment theory procedure was only partially successful in averaging over these fluctuations which resulted in a $\pm 10\%$ uncertainty in the final widths.

The physical width of the $1\sigma_u^2 \ ^1\Sigma_g^+$ autoionizing state was determined at each R value by evaluating $\Gamma(E, R)$ at the resonance energy, which, in turn, was calculated from the relationship¹

$$E_r - E_Q - \Delta(E_r) = 0. \quad (1)$$

Here, E_Q is the "unshifted" resonance energy, i.e., the eigenvalue of $Q_0 H Q_0$, and $\Delta(E)$ is the energy shift of the resonance due to its coupling to the non-resonant background. Since the $1\sigma_u^2$ resonance is quite broad for $R > 1.4a_0$, it was necessary to evaluate $\Delta(E)$ explicitly to obtain an accurate resonance energy E_r . For a neutral molecule $\Delta(E)$ is given by

$$\Delta(E) = \sum_n \frac{|\langle \phi_r | H | P\Psi_n \rangle|^2}{E - \epsilon_n} + \frac{1}{2\pi} \mathcal{P} \int_{\epsilon_{\text{ion}}}^{\infty} d\epsilon \frac{\Gamma(\epsilon)}{E - \epsilon}, \quad (2)$$

where the sum over n runs over the bound solutions of PHP , each with a wave function $P\Psi_n$ and energy ϵ_n . In the present case, these solutions represent the $X^1\Sigma_g^+$ ground state and the $^1\Sigma_g^+$ Rydberg states converging to the ground $^2\Sigma_g^+$ state of H_2^+ . The second term in Eq. (2) involves a principal-value integral provided E is greater than the ionization threshold ϵ_{ion} . Of course, all of the quantities appearing in Eq. (2) depend on the internuclear distance. The matrix elements $\langle \phi_r | H | P\Psi_n \rangle$ and the eigenvalues ϵ_n were

taken directly from the CI calculations. The principal-value integral was evaluated by quadrature using Simpson's rule and a technique that Heller and Reinhardt²⁰ devised for the proper handling of the singularity. For $\Gamma(E)$ we used the analytic representations¹⁹ of the widths in terms of inverse powers of E . Since our orbital basis was chosen to provide reasonable approximations to the widths only for ejected electron energies less than 15 eV, we used an arbitrary, but reasonable, asymptotic form $\Gamma(E) = C/E$ for larger energies. The constant C was determined by requiring $\Gamma(E)$ to be continuous at a suitable value of E .

Tables I and II summarize our calculated resonance energies and widths of the $1\sigma_u^2 \ ^1\Sigma_g^+$ state and compare them with some of the previous results. Figures 2 and 3 show more completely the internuclear distance dependence of the potential-energy curves and of the resonance widths obtained in the various calculations. A comparison of the present results obtained with CI-A and CI-B shows that including the $1\sigma_g^2$ configuration in the resonance subspace significantly raises the potential-energy curve of the $1\sigma_u^2$ doubly excited state at large internuclear distances, e.g., by 2 eV at $R = 4.0a_0$, if the energy shift is neglected (see Table I). However, the two different choices of projection operators give the same resonance energy within 0.001 hartree when the shift is included. This result provides direct numerical verification of the formal assertion¹ that the true resonance energy is independent of the definition of the resonant subspace, provided P and Q are internally consistent and the shift is properly evaluated. Thus, the nonuniqueness of the resonant subspace does not lead to any uncertainty in the final resonance position. Furthermore, as Table II shows, changing the choice of projection operators

TABLE I. Comparison of calculated energies (in hartree) of the $1\sigma_u^2 \ ^1\Sigma_g^+$ state of H_2 .

Calculation	$R(a_0)$				
	1.4	2.0	2.5	3.0	4.0
Present					
CI-A (without shift)	-0.1046	-0.3975	-0.5404	-0.6308	-0.7251
CI-B (without shift)	-0.1013	-0.3859	-0.5165	-0.5899	-0.6429
CI-A or -B (with shift)	-0.102	-0.399	-0.545	-0.651	-0.702
Rydberg-state analysis			-0.5601	-0.6435	
Bottcher and Docken ^a	-0.0999	-0.3900	-0.5320	-0.6223	-0.7175
Moiseyev and Corcoran ^b	-0.0967				

^aReference 2.

^bReference 9.

TABLE II. Comparison of calculated widths (in eV) of the $1\sigma_u^2 1\Sigma_g^+$ state of H_2 .

Calculation	$R(a_0)$		
	1.4	2.0	2.5
Present CI-A	0.69	1.32	1.74
Present CI-B	0.65	1.25	1.68
Bottcher and Docken ^a	0.97	0.98	0.44
Moiseyev and Corcoran ^b	1.21		
Robb ^c	0.65	1.34	1.83 ^d

^aReference 2.

^bReference 9.

^cReference 5.

^dValue interpolated to $R = 2.5a_0$.

changes the calculated widths by at most 6%, which is smaller than the overall 10% uncertainty arising from the Stieltjes procedure.

Previous theoretical studies of the $1\sigma_u^2 1\Sigma_g^+$ autoionizing state fall into two groups: Those which used discrete basis-set techniques to calculate the resonance parameters directly and those which extracted these parameters from the results of scatter-

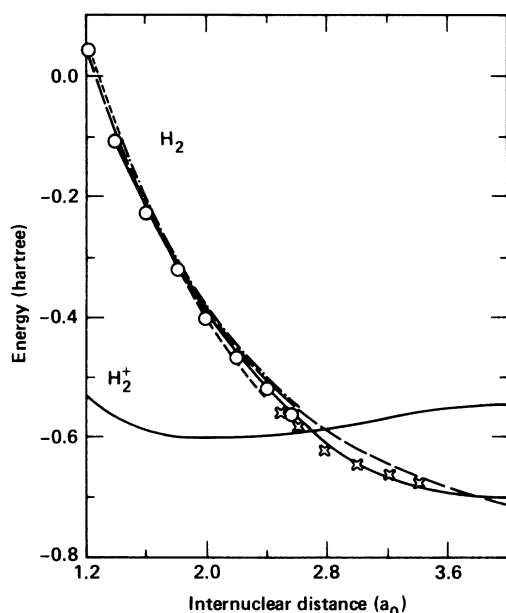


FIG. 2. Comparison of the calculated potential-energy curves of the $1\sigma_u^2 1\Sigma_g^+$ doubly excited state of H_2 . (—) present Stieltjes results, (×) present Rydberg-state analysis, (---) Bottcher and Docken (Ref. 2), and Collins and Schneider (Ref. 7), (- · -) Robb (Ref. 5), (- - -) Takagi and Nakamura (Ref. 6); (○) Sato and Hara (Ref. 4); the ground $2\Sigma_g^+$ state of H_2^+ is also shown.

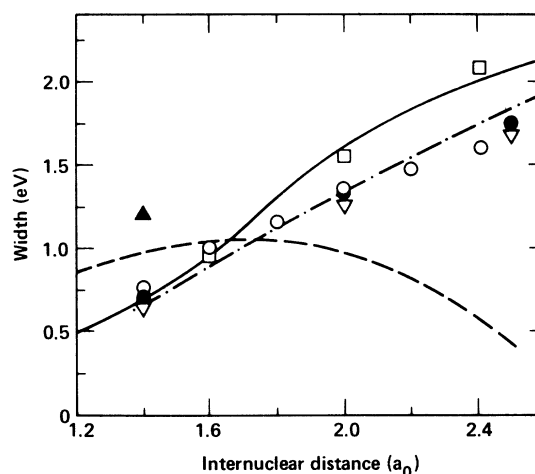


FIG. 3. Comparison of the calculated widths of the $1\sigma_u^2 1\Sigma_g^+$ doubly excited state of H_2 . (●) present CI-A, (▽) present CI-B, (▲) Moiseyev and Corcoran (Ref. 9), (—) Bottcher and Docken (Ref. 2), (- · -) Robb (Ref. 5), (- - -) Takagi and Nakamura (Ref. 6), (○) Sato and Hara (Ref. 4), (□) Collins and Schneider (Ref. 7).

ing calculations on the $e^- + H_2^+$ system. The first group includes the work of Bottcher and Docken,² Moiseyev and Corcoran,⁹ and Sato and Hara⁴ whereas the unpublished study of Robb⁵ and the recent calculations of Takagi and Nakamura⁶ and of Collins and Schneider⁷ are in the second group. Bottcher and Docken² used the same definition of the projection operators, and of the resonance subspace, as we did in the CI-A calculations. As Table I and Fig. 2 show, our unshifted energies obtained with CI-A are very close to, but slightly lower than, their values.² On the other hand, both the magnitude and the R dependence of the widths obtained in the present work (as well as in the electron-scattering calculations⁵⁻⁷) differ significantly from those reported by Bottcher and Docken² (see Table II and Fig. 3). This discrepancy is probably due to numerical errors and/or the use of undistorted Coulomb waves to represent the ejected electron in the earlier calculations.² Moiseyev and Corcoran employed the method of complex scaling to compute the complex energy of the $1\sigma_u^2$ resonance at $R = 1.4a_0$. Their resonance energy is 0.2 eV higher than our CI-A value, and their width is almost a factor of 2 too high. These differences can be attributed to the relatively small orbital basis set and CI space (only 45 configurations) employed in the complex-scaling calculations.⁹ As Fig. 2 shows, our calculated potential-energy curve is in good agreement with that obtained by Sato and Hara.⁴ [We

plotted the energies that Sato and Hara obtained without the shift because their calculated shift is much too negative due to the neglect of the bound, Rydberg-state contribution to Eq. (2).] The resonance widths also agree quite well, although our $\Gamma(R)$ increases somewhat more slowly at larger R values (see Fig. 3).

With respect to the electron-scattering calculations, our resonance widths agree very well with the values of Robb,⁵ who studied the elastic scattering of electrons from $H_2^+ \ ^2\Sigma_g^+$ using a two-state close-coupling approximation and a spherical partial-wave expansion (see Table II and Fig. 3). Equally good agreement was found earlier^{11,12} in the case of the $1\sigma_u 2\sigma_g \ ^1\Sigma_u^+$ and $1\sigma_u 1\pi_g \ ^1\Pi_u$ doubly excited states. Takagi and Nakamura^{6,21} have also done elastic scattering calculations but used the Kohn variational method and a spheroidal partial-wave expansion instead. Because they included a large number of discrete, two-electron configurations in their trial wave functions, their potential-energy curve is comparable in accuracy to those obtained in purely L^2 -type calculations, as shown in Fig. 2. The widths determined by Takagi and Nakamura⁶ also agree with Robb's and our values between $R = 1.2a_0$ and $1.5a_0$, however, their results are significantly higher than ours at larger internuclear distances as shown in Fig. 3. Very recently, Collins and Schneider⁷ performed two- and four-state close-coupling calculations of the $e + H_2^+$ system using a linear algebraic approach. Their resonance energies fall between our results and the earlier data of Robb.⁵ For $R < 2.4a_0$, the potential-energy curve obtained by Collins and Schneider is the same, within graphical accuracy, as that of Bottcher and Docken,² and hence it is not shown separately in Fig. 2. The widths calculated by Collins and Schneider⁷ are quite close to those of Takagi and Nakamura⁶ but are 20% higher than the Stieltjes results at $R \geq 2a_0$. Since all of the recently calculated widths⁴⁻⁷ agree closely at smaller internuclear distances, the discrepancies observed at large R values are puzzling. These differences may be due to the different treatments of partial-wave (primarily s - d) or channel coupling and of electron polarization effects in the present work and in the electron-scattering calculations employing spherical⁷ and spheroidal⁶ angular expansions.

III. $^1\Sigma_g^+$ RYDBERG-STATE PERTURBATIONS

The interaction between Rydberg and non-Rydberg configurations among excited molecular states leads to level perturbations, autoionization, and predissociation of many high-Rydberg levels.

In the $^1\Sigma_g^+$ manifold of H_2 , this interaction is seen even in the first excited state. Unfortunately, these states are not easily accessible by single-photon absorption from the ground state. Although some experimental evidence is available from emission spectroscopy and from multiphoton absorption, these data are sparse in comparison with those available for other symmetries. Thus, our analysis is based on the *ab initio* potential-energy curves for the *EF* and *GK* states from Wolniewicz and Dressler.²² Comparison of their predicted energy levels²³ with experiment shows that the *EF* and *GK* curves are of very high accuracy, with errors of a few meV. The same paper²² also reported calculations of the *H \bar{H}* curves which were apparently less accurate than the *EF* and *GK* potentials.

Let us suppose that the electronic wave functions describing the excited $^1\Sigma_g^+$ states can be expressed as linear combinations

$$\psi(q, R) = \frac{1}{N(R)} \left[\phi_d(q, R) + \sum_{n,l} a_{nl}(R) \psi_{nl}(q, R) \right] \quad (3)$$

in which $\phi_d(q, R)$ represents the doubly excited configuration $1\sigma_u^2$ and the $\psi_{nl}(q, R)$ represent Rydberg configurations $1\sigma_g n\sigma_g$. We will assume that the contributions from the higher doubly excited configurations and from the ground state $X \ ^1\Sigma_g^+$ are negligible. The symbol q is used to indicate the coordinates of both electrons. The potential-energy curves are then obtained as eigenvalues of the electronic Hamiltonian

$$[H_{el} - E(R)]\psi(q, R) = 0. \quad (4)$$

Let us define the matrix elements

$$E_d(R) = \langle \phi_d(q, R) | H_{el} | \phi_d(q, R) \rangle, \quad (5)$$

$$V_{nl}(R) = \langle \phi_d(q, R) | H_{el} | \psi_{nl}(q, R) \rangle \quad (6)$$

and let us assume that H_{el} is diagonal within the subspace spanned by the Rydberg states, i.e.,

$$\langle \psi_{nl}(q, R) | H_{el} | \psi_{n'l'}(q, R) \rangle = E_{nl}(R) \delta_{nn'} \delta_{ll'}. \quad (7)$$

The mixing coefficients a_{nl} can then be obtained by premultiplication of Eq. (2) by $\phi_d^*(q, R)$ or $\psi_{n,l}^*(q, R)$ and integration over the electronic coordinates. This gives

$$E_d(R) + \sum_{n,l} V_{nl}(R) a_{nl}(R) = E(R) \quad (8)$$

and

$$V_{nl}^*(R) + E_{nl}(R) a_{nl}(R) = E(R) a_{nl}(R). \quad (9)$$

The potential curves for the mixed states are then given by

$$E(R) = E_d(R) + \sum_{n,l} |V_{nl}(R)|^2 [E(R) - E_{nl}(R)]^{-1}. \quad (10)$$

If $V_{nl}(R)$ and $E_{nl}(R)$ are known, the eigenvalues can be located rapidly by a numerical search procedure, since the position of the singularities on the right-hand side (rhs) gives both upper and lower bounds for most of the roots. Our problem is to invert this procedure and deduce the values of these matrix elements from the potential-energy curves $E(R)$ calculated by Wolniewicz and Dressler.²² In order to do this, we must parametrize the matrix elements.

Since the $1\sigma_u$ orbital is dominated by the p -wave component and we are primarily interested in the lowest three excited states, it seems reasonable to include Rydberg configurations with $l=0$ and 2 and to neglect those with $l \geq 4$. The n dependence of the matrix elements can best be expressed through the quantum defects $\mu_l(R)$. Denoting the potential curve for the ground state of H_2^+ by $E^+(R)$, we write

$$E_{nl}(R) = E^+(R) - \frac{1}{2[n - \mu_l(R)]^2}. \quad (11)$$

Since the configuration mixing elements $V_{nl}(R)$ are dominated by short-range interactions, their n dependence is given approximately by

$$V_{nl} = \frac{v_l}{[n - \mu_l(R)]^{3/2}}. \quad (12)$$

The quantum defects $\mu_l(R)$ were taken as quadratic functions of R , with arbitrary coefficients, and the energy of the $1\sigma_u^2$ configurations was set as

$$E_d(R) = AR \exp(-BR) - R^{-1} - 0.5094. \quad (13)$$

This form was chosen so that the curve joins smoothly to that of H^+-H^- at large R , but this long-range behavior is of no consequence to our conclusions.

Our best fit to the EF and GK states is shown in Fig. 4. For separations between $2.5a_0$ and $3.5a_0$ the largest discrepancy is $\sim 6 \times 10^{-4}$ a.u. (15 meV). This fit is obtained with $v_0 = 0.048$, $v_2 = 0.08$, $A = 5.7936$, $B = 1.49$,

$$\begin{aligned} \mu_0(R) = & -0.1335 - 0.0675(R - 2.5) \\ & + 0.019(R - 2.5)^2, \end{aligned} \quad (14)$$

and

$$\begin{aligned} \mu_2(R) = & 0.055 + 0.048(R - 2.5) \\ & + 0.05(R - 2.5)^2. \end{aligned} \quad (15)$$

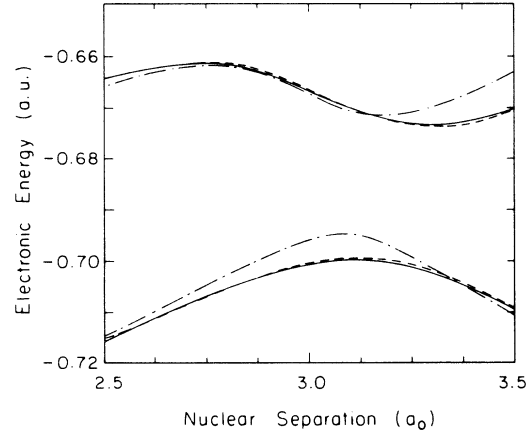


FIG. 4. Potential curves for the EF and GK states of H_2 : (—) Dressler and Wolniewicz, (---) best fit as described in Sec. III, (-·-) calculated using the CI matrix elements obtained in Sec. II.

After this fit was completed, we learned of more accurate *ab initio* calculations by Wolniewicz and Dressler²⁴ on the HH potential. In Table III, the new results are compared with the values given in Ref. 22 and the energy predicted by Eq. (10). The close agreement between the improved *ab initio* calculation and our predictions increases our confidence in the model, especially in the region of strong configuration mixing, $2.5 \leq R \leq 3.25a_0$.

Knowledge of the variation of the quantum defects with R is important for studies of vibrational autoionization of the high-Rydberg states, as discussed in a subsequent paper.¹³ Here our major purpose is to study the energy and width of the $1\sigma_u^2$ state. As can be seen from Fig. 2, the potential curve $E_d(R)$ agrees well with an extrapolation of the algebraic variational results of Takagi and Nakamura,⁶ but it has a slightly different slope than our *ab initio* curve including the energy shift. The stabilization point R_s is found to be close to $2.65a_0$.

The autoionization width can be estimated, since the wave functions describing the scattering of low-energy electrons by H_2^+ molecules are very similar in shape to those of the high-Rydberg states. Using a zeroth-order quantum-defect extrapolation, we find

$$\Gamma = 2\pi(v_0^2 + v_2^2) = 0.055 \text{ a.u. (1.5 eV)}.$$

The corresponding value obtained from the Stieltjes moment calculation of Sec. II is 0.053 a.u. However, the agreement with respect to the partial widths is not so good. Our Rydberg-state analysis suggests that the ratio of the d - and s -wave contributions is ~ 2.8 , which seems to be significantly smaller²⁵ than

TABLE III. Potential curve for the $H\bar{H}$ state of H_2 .

	$R(a_0)$				
	2.5	2.75	3.0	3.25	3.5
<i>Ab initio</i> ^a	-0.6437	-0.6329	-0.6276	-0.6224	-0.6162
Model eigenvalue	-0.6454	-0.6376	-0.6306	-0.6248	-0.6190
<i>Ab initio</i> ^b	-0.6450	-0.6373	-0.6305	-0.6244	-0.6178

^aReference 22.^bReference 24.

the value suggested by the Stieltjes method. In order to illustrate this difference, we have computed the *EF* and *GK* potential curves that result when the matrix elements $V_{nl}(R)$ describing the configuration interaction are replaced by the values computed in Sec. II. As can be seen from Fig. 4, the two adiabatic curves approach more closely due to the reduction in the strength of the coupling between the doubly excited configuration and the $1\sigma_g 2s\sigma_g$ Rydberg state.

IV. SUMMARY AND CONCLUSIONS

By using the Stieltjes moment theory method, we have shown that the electronic matrix element which controls the autoionization width of the $1\sigma_u^2 {}^1\Sigma_g^+$ state of H_2 is sensitive to the energy of the ejected electron as well as the internuclear distance. When the energy dependence is taken into account, the strength of the CI responsible for autoionization is consistent with the values deduced from an analysis of the double minima in the potential-energy curves of the ${}^1\Sigma_g^+$ Rydberg states of H_2 . However, there remains some uncertainty in the relative magnitude of the coupling between the $1\sigma_u^2$ configuration and the $s\sigma$ and $d\sigma$ manifolds.

These calculations suggest that the use of energy-dependent, nonlocal widths is worthwhile in subsequent theoretical studies of resonance scattering in $e\text{-}H_2^+$ collisions. The local width, obtained by evaluating the autoionization matrix elements at the

resonance energy, is a monotonically increasing function of the internuclear separation. Our values for the local width are consistent with those obtained independently by Robb,⁵ Sato and Hara,⁴ Takagi and Nakamura,⁶ and Collins and Schneider.⁷ There remains some discrepancy between the widths obtained with bound-state techniques^{4,10-12} and those extracted from electron-scattering calculations^{6,7} for $R \geq 2.0a_0$.

By evaluating the shift of the $1\sigma_u^2$ configuration from the energy-dependent -autoionization matrix elements, we have shown that, within our numerical accuracy, the resonance energy is independent of the particular projection operator used to define the resonance. The potential-energy curve of the $1\sigma_u^2$ state appears to cross the ground state of H_2^+ between $2.6a_0$ and $2.7a_0$. Our Rydberg-state analysis suggests a crossing point close to $2.65a_0$.

ACKNOWLEDGMENTS

We thank Dr. W. D. Robb, Dr. H. Takagi, Dr. H. Nakamura, Dr. M. Sato, Dr. S. Hara, Dr. L. A. Collins, Dr. B. I. Schneider, Dr. K. Dressler, and Dr. P. Quadrelli for sending us their results prior to publication. Part of this work was supported by the National Science Foundation under Grant No. PHY-81-05074 and part of it was performed under the auspices of the U.S. Department of Energy by the Lawrence Livermore National Laboratory under Contract No. W-7405-ENG-48.

¹H. Feshbach, Ann. Phys. (N.Y.) **19**, 287 (1962).²C. Bottcher and K. Docken, J. Phys. B **7**, L5 (1974).³K. Rai Dastidar and T. K. Rai Dastidar, J. Phys. Soc. Jpn. **46**, 1288 (1979).⁴H. Sato and S. Hara (private communication). For a similar calculation on He_2^{2+} , see J. Phys. B **13**, 4577 (1980).⁵W. D. Robb (private communication).⁶H. Takagi and H. Nakamura, in *Abstracts of the XII International Conference on the Physics of Electronic and Atomic Collisions, Gatlinburg, Tennessee, 1981*, edited by S. Datz (North-Holland, Amsterdam, 1981), p. 457, and private communication.⁷L. A. Collins and B. I. Schneider, Phys. Rev. A **27**, 101 (1983).⁸B. R. Junker, Adv. At. Mol. Phys. (in press).

- ⁹N. Moiseyev and C. Corcoran, *Phys. Rev. A* **20**, 814 (1979).
- ¹⁰A. U. Hazi, *J. Phys. B* **11**, L259 (1978).
- ¹¹A. U. Hazi, in *Electron-Molecule and Photon-Molecule Collisions*, edited by T. Rescigno, V. McKoy, and B. Schneider (Plenum, New York, 1979), p. 281.
- ¹²A. U. Hazi, in *Electron-Atom and Electron-Molecule Collisions*, edited by J. Hinze (Plenum, New York, 1983), p. 103.
- ¹³A. Giusti, J. N. Bardsley, and C. Derkits, *Phys. Rev. A* (in press).
- ¹⁴K. Kirby, S. Guberman, and A. Dalgarno, *J. Chem. Phys.* **70**, 4635 (1979).
- ¹⁵W. Kolos and L. Wolniewicz, *J. Chem. Phys.* **43**, 2429 (1965).
- ¹⁶The s -function with exponent 0.015 was not included because a very similar orbital already appeared in the $7\sigma_g$ set.
- ¹⁷In practice, even a two-configuration wave function is not sufficient since the $1s$ orbitals in $H\,1s$ and H^-1s^2 are not the same. Consequently, additional configurations must be included to describe correctly the two dissociation limits: $H\,1s + H\,1s$ and $H^+ + H^-1s^2$.
- ¹⁸P. J. Langhoff, *Int. J. Quant. Chem. Symp.* **8**, 347 (1974).
- ¹⁹A. U. Hazi and T. N. Rescigno, *Phys. Rev. A* **16**, 2376 (1977).
- ²⁰E. J. Heller and W. P. Reinhardt, *Phys. Rev. A* **7**, 365 (1973).
- ²¹H. Takagi and H. Nakamura, *J. Phys. B* **13**, 2619 (1980).
- ²²L. Wolniewicz and K. Dressler, *J. Mol. Spectrosc.* **67**, 416 (1977).
- ²³K. Dressler, R. Galluser, P. Quadrelli, and L. Wolniewicz, *J. Mol. Spectrosc.* **75**, 205 (1979).
- ²⁴L. Wolniewicz and K. Dressler, *J. Mol. Spectrosc.* **77**, 286 (1979).
- ²⁵P. Quadrelli and K. Dressler have performed an independent deperturbation analysis of the EF , GK , and $H\bar{H}$ curves and find the ratio of d - to s -wave components of Γ to be close to two.